

# Photonic-bandgap planar hollow waveguide

Andrei B. Fedotov, Aleksandr N. Naumov, Dimitrii A. Sidorov-Biryukov, Nikolai V. Chigarev,  
and Aleksei M. Zheltikov

*International Laser Center, Faculty of Physics, Moscow State University, Moscow 119899, Russia*

Joseph W. Haus

*Electro-Optics Program, University of Dayton, Dayton, Ohio 45469-0245*

Richard B. Miles

*Department of Mechanical and Aerospace Engineering, Princeton University, Princeton, New Jersey 08544-5263*

Received May 29, 2001; revised manuscript received November 1, 2001

A combination of a diffraction grating and a mirror integrates a hollow waveguide and a photonic-bandgap structure into a compact optical element, offering a simple new structure for various applications in nonlinear and ultrafast optics. The main features of transmission spectra observed in experiments performed with such waveguide structures are qualitatively interpreted in terms of the coupled-mode theory. Localization of light near the surface of a metal-coated grating in lowest-order TM modes in the created waveguide enhances effects related to the photonic-bandgap structure. © 2002 Optical Society of America

OCIS codes: 230.7390, 260.2030.

## 1. INTRODUCTION

Photonic-bandgap (PBG) structures are extensively employed nowadays for both fundamental research and creation of practical optical components.<sup>1–3</sup> Numerous applications of such structures are based on their reflection, transmission, and dispersion properties, related to the existence of photonic bandgaps (PBGs) in their transmission spectra and dispersion relations. A high reflection coefficient provided by a PBG underlies the operation of such widespread optical components as multilayer coatings,<sup>4</sup> Bragg reflectors,<sup>5,6</sup> periodic waveguides,<sup>7,8</sup> and narrow-band filters.<sup>8,9</sup> Other optical devices make use of remarkable dispersion properties of periodic multilayers to produce ultrashort pulses and control their parameters,<sup>10–12</sup> slow down light pulses in a controllable fashion,<sup>13</sup> achieve phase and group-velocity matching in nonlinear-optical interactions,<sup>14,15</sup> implement optical switching and logic gating,<sup>16–20</sup> and perform many other functions. Multilayer structures with spatially modulated unit-cell sizes (chirped mirrors)<sup>21–26</sup> have promoted impressive progress in the generation of extremely short light pulses in recent years. Mirrors of this type are used nowadays not only as intracavity elements, but also as extracavity components allowing efficient compression of chirped light pulses to femtosecond pulse durations.<sup>10,11</sup>

A parallel trend in the development of ultrafast nonlinear optics involves the use of hollow fibers for the generation of very short light pulses and frequency upconversion.<sup>27–31</sup> Gas-filled hollow fibers have been recently shown to allow extremely short light pulses to be produced through self-phase modulation,<sup>27,28</sup> high-order harmonic generation to be enhanced due to the increase in the interaction length and improved phase matching,<sup>29–31</sup>

and the sensitivity of gas-phase analysis based on nonlinear-optical spectroscopic techniques to be improved.<sup>32,33</sup>

The main idea of our study is to integrate a hollow waveguide and a PBG structure into a compact optical component. Guided by this idea, we created an optical element consisting of a diffraction grating and a mirror (or another diffraction grating). The possibility of creating a one-dimensional PBG structure based on a grating pair has been previously discussed by Todor and Hayase.<sup>34</sup> The results of transmission measurements performed<sup>34</sup> on a grating pair were interpreted with the use of a simple formula for a one-dimensional PBG structure completely ignoring waveguiding effects. We show below that the waveguiding properties of a grating-mirror PBG structure play a very important role, having a noticeable influence on the transmission and dispersion of such a structure and considerably extending its filtering and phase-matching capabilities.

The results of our experiments presented in this paper demonstrate that a grating-mirror PBG structure, in fact, displays many properties inherent in a planar corrugated waveguide. In particular, photonic bandgaps arise in the dispersion relation and transmission spectra of this structure due to a strong coupling of forward and backward waves within certain frequency ranges.<sup>8</sup> However, in contrast to a conventional corrugated waveguide, the light is guided in a gas (or whatever fills the gap between the grating and the mirror) in our structure, which is reminiscent of the situation encountered in gas-filled hollow fibers. Similar to gas-filled hollow fibers, the created waveguide structure allows the waveguiding of high-intensity laser pulses and seems to offer much promise for

many applications, including pulse compression, harmonic generation, and gas-phase analysis based on nonlinear spectroscopy. Periodic perturbation of the refractive index introduced by the grating, giving rise to photonic bandgaps, provides additional degrees of freedom in tuning the dispersion of the structure, opening new ways of phase and group-velocity matching of light pulses and appealing for soliton research. We anticipate that the efficiency of nonlinear optical processes can be enhanced in such waveguides due to the local-field enhancement, which is characteristic of PBG structures. Finally, localization of light near a metal-coated grating surface in lowest-order TM modes in the created waveguide allows effects related to the photonic-bandgap structure to be effectively enhanced.

## 2. BASIC PROPERTIES OF A PLANAR PBG HOLLOW WAVEGUIDE

To illustrate the main properties of a planar hollow waveguide consisting of a diffraction grating and a mirror (Fig. 1), we employ a standard approach based on couple-mode equations.<sup>8</sup> Within the framework of this approach, a periodic modulation of the refractive index introduced by the grating is treated as a perturbation that couples forward and backward modes of an unperturbed waveguide. Around Bragg resonances, this coupling is especially strong, giving rise to photonic bandgaps. The electric field inside a corrugated planar waveguide can be then represented as a superposition of modes of an unperturbed planar waveguide with unknown slowly varying envelopes<sup>8</sup>:

$$\mathbf{E} = 1/2 \sum_n \mathbf{f}_n(x) [A_n(z) \exp(i\beta_n z) + B_n(z) \exp(-i\beta_n z)] \exp(-i\omega t) + \text{c.c.}, \quad (1)$$

where  $\omega$  is the radiation frequency;  $\beta_n$  and  $\mathbf{f}_n(x)$  are the propagation constant and the transverse field distribution for the  $n$ th mode of the planar waveguide, respectively;  $A_n(z)$  and  $B_n(z)$  are the slowly varying envelopes of the forward and backward waveguide modes (orientation of the coordinate axes is shown in Fig. 1).

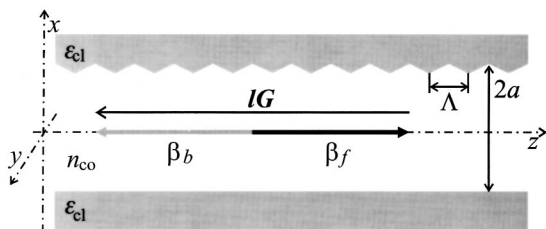


Fig. 1. Mirror and diffraction grating combined to form a planar hollow corrugated waveguide:  $\Lambda$  is the period of the grating,  $2a$  is the separation between the grating and the mirror,  $n_{\text{co}}$  is the refractive index of the waveguiding layer, and  $\epsilon_{\text{cl}}$  is the dielectric constant of the cladding. The photonic bandgap in the dispersion relation and transmission spectrum of such a structure arises due to a strong coupling of forward and backward waveguide modes with propagation constants  $\beta_f$  and  $\beta_b$ , with the reciprocal lattice constant  $G$  involved in momentum conservation, leading to a Bragg resonance of Eq. (7).

Perturbation of the dielectric function  $\Delta\epsilon(x, z)$  due to the spatial modulation introduced by the grating gives rise to an additive to the polarization equal to

$$\tilde{\mathbf{P}} = \Delta\epsilon(x, z)\mathbf{E}. \quad (2)$$

Whenever  $\Delta\epsilon(x, z)$  is a scalar quantity, no coupling between TE and TM modes arises, and TE and TM modes are coupled in an independent way.<sup>8</sup> Since the perturbation introduced by a diffraction grating in the case under study is periodic along the  $z$  axis, this perturbation can be expanded as a Fourier series:

$$\Delta\epsilon(x, z) = \sum_l \tilde{\epsilon}_l(x) \exp(ilGz), \quad (3)$$

where  $G = 2\pi/\Lambda$  is the reciprocal lattice constant and  $\Lambda$  is the period of the grating.

The set of equations for the amplitudes of coupled modes is then written as<sup>8</sup>

$$\frac{dA_n}{dz} = \sum_{m,l} \alpha_{nml} \{A_m \exp[i(\beta_m - \beta_n + lG)z] + B_m \exp[-i(\beta_m + \beta_n - lG)z]\}, \quad (4)$$

$$\frac{dB_n}{dz} = -\sum_{m,l} \alpha_{nm-l} \{A_m \exp[i(\beta_m + \beta_n - lG)z] + B_m \exp[-i(\beta_m - \beta_n + lG)z]\}, \quad (5)$$

where

$$\alpha_{nml} = i \frac{2\pi\omega^2}{\beta_n c^2} \frac{\int \tilde{\epsilon}_l(x) \mathbf{f}_m(x) \mathbf{f}_n^*(x) dx}{\int |\mathbf{f}_n(x)|^2 dx}. \quad (6)$$

With  $\alpha_{fbl} \neq 0$ , a forward mode with a mode index  $f$  and a backward mode with a mode index  $b$  are especially strongly coupled when the Bragg-resonance condition,

$$\beta_f + \beta_b = lG, \quad (7)$$

where  $l$  is an integer, is satisfied. In this regime, an efficient energy exchange between forward and backward modes occurs in a corrugated planar waveguide.

Figure 2 gives a general idea of how the photonic bandgap is produced in a corrugated planar hollow waveguide. Many waveguide modes were simultaneously excited in PBG waveguides studied in our experiments, where structures with large air gaps between the grating and the mirror (with the grating-mirror separation  $d = 2a$  in the range 20–100  $\mu\text{m}$ ) were used. In such a situation, a photonic bandgap is a result of overlapping of photonic bandgaps, corresponding to a family of strongly coupled modes meeting the Bragg-resonance condition of Eq. (7). Figure 2 also shows the effective refractive index for the waveguide propagation regime, defined as  $n_{\text{eff}} = \tilde{\beta}_n/k$ , where  $\tilde{\beta}_n$  is the propagation constant of the  $n$ th mode in the corrugated planar waveguide. This effective refractive index provides an idea of the phase velocities of the coupled modes, allowing phase-matching abilities of the created PBG waveguide to be understood.

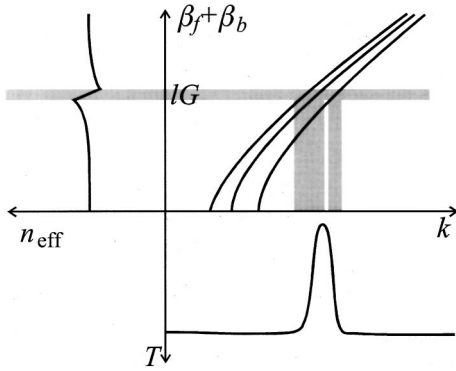


Fig. 2. Dispersion relations, effective refractive index, and the photonic bandgap for a planar hollow PBG waveguide: photonic bandgaps corresponding to a family of strongly coupled modes meeting the Bragg-resonance condition of Eq. (7) overlap to form a broad photonic bandgap. The effective refractive index  $n_{\text{eff}} = \tilde{\beta}_n/k$ , where  $\tilde{\beta}_n$  is the propagation constant of the  $n$ th waveguide mode in the corrugated planar waveguide, provides an idea of the phase velocities of the coupled modes and allows phase-matching capabilities of the PBG waveguide to be analyzed.

### 3. MODE COUPLING IN A METAL-COATED PLANAR PBG WAVEGUIDE

As can be seen from Eqs. (4)–(6), the coupling of modes in a corrugated waveguide depends on the light-field distributions and propagation constants for the modes of an unperturbed waveguide. Analysis of the modes of an unperturbed waveguide is therefore of key importance for understanding the properties of mode coupling and dispersion of waveguide modes in a PBG waveguide. Many important properties of modes in waveguides consisting of a metal-coated grating and a mirror (Fig. 1) studied in our experiments (see Section 4) are associated with the character of the dielectric function of a metal covering the surface of the grating. In particular,  $TM_0$  and  $TM_1$  modes in such a waveguide are symmetric and antisymmetric superpositions of surface waves existing on metal–dielectric interfaces.<sup>35</sup> In the limiting case when

$$ka \gg 1, \tag{8}$$

$TM_0$  and  $TM_1$  modes of a metal-coated planar waveguide have equal propagation constants, coinciding with the propagation constant for a surface wave,<sup>35</sup>

$$\beta_n = k \sqrt{\frac{n_{\text{co}}^2 \epsilon_{\text{cl}}}{n_{\text{co}}^2 + \epsilon_{\text{cl}}}}. \tag{9}$$

Note that the propagation constant for such modes is given by a complex quantity whose real part exceeds the phase velocity for a free gas at the same frequency. The transverse distributions of the electric-field projections on the  $x$  axis in the  $TM_0$  and  $TM_1$  modes of a metal-coated waveguide are described by the expressions<sup>35</sup>

$$[f_0(x)]_x \approx \cosh[u'x/a], \tag{10}$$

$$[f_1(x)]_x \approx \sinh[u'x/a], \tag{11}$$

respectively, where

$$u' = k \sqrt{\frac{n_{\text{co}}^2 \epsilon_{\text{cl}}}{n_{\text{co}}^2 + \epsilon_{\text{cl}}} - 1}. \tag{12}$$

For all the other TM modes far from the cut-off region, where the condition

$$\frac{u_n}{ak} \ll 1 \tag{13}$$

is satisfied, the eigenvalue of the  $n$ th mode can be written as<sup>35,36</sup>

$$u_n \approx (n + 1) \frac{\pi}{2} [1 - (ka \eta \sqrt{1 - \epsilon_{\text{cl}} n_{\text{co}}^{-2}})^{-1}]. \tag{14}$$

Here,  $\epsilon_{\text{cl}}$  is the dielectric function of the metal,  $n_{\text{co}}$  is the refractive index of the waveguiding layer (air), and  $\eta = n_{\text{co}}^2/\epsilon_{\text{cl}}$  for TM modes and  $\eta=1$  for TE modes. The propagation constant in this case is given by

$$\beta_n \approx k - \frac{[(n + 1)\pi]^2}{8ka^2} \tag{15}$$

for both TM and TE modes of the planar waveguide. Phase-matching conditions (7) are, therefore, identical for TE and TM modes in this case. However, the coupling coefficients  $\alpha_{nml}$  are different for TE and TM modes because the fields of the TE and TM modes differ considerably from each other near the corrugated surface. We employ the following expressions for the transverse field distribution in the waveguiding layer for both TM and TE modes<sup>36</sup>:

$$\mathbf{f}_n(x) \approx \cos[u_n x/a], \tag{16}$$

for even  $n$  and

$$\mathbf{f}_n(x) \approx \sin[u_n x/a] \tag{17}$$

for odd  $n$ . In the case of TE modes, the electric field is directed along the  $y$  axis. The electric field in TM modes has nonzero projections on the  $x$  and  $z$  axes, with  $|[f_n(x)]_x| \gg |[f_n(x)]_z|$  for a metal-coated planar waveguide with  $|\sqrt{\epsilon_{\text{cl}}}| \gg n_{\text{co}}$ .

Field distributions for several TE and TM modes for radiation with a wavelength  $\lambda=0.62 \mu\text{m}$  in a planar waveguide with aluminum walls and a half-width  $a = 11 \mu\text{m}$  calculated with the use of Eqs. (10)–(12), (14), (16), and (17) are shown in Fig. 3. As can be seen from this figure, much of the radiation energy of the surface  $TM_0$  and  $TM_1$  modes is concentrated within the area of the perturbed dielectric function [the hatched areas in Figs. 3(a) and 3(b)]. For all the other waveguide modes, the fraction of radiation energy concentrated within the area of the perturbed dielectric function increases with the growth in the mode index [which is equal, by its definition, to the number of field zeros in the waveguiding layer; see Fig. 3(a), where the transverse distributions for  $TE_0$  and  $TE_7$  waveguide modes are shown]. Consequently, especially large coupling coefficients  $\alpha_{nml}$  are achieved in the case of a corrugated waveguide when either both forward and backward coupled modes or at least one of these modes is a surface  $TM_0$  or  $TM_1$  mode.

Except for the case of surface TM modes, the coupling coefficients of TM and TE modes increase with the growth

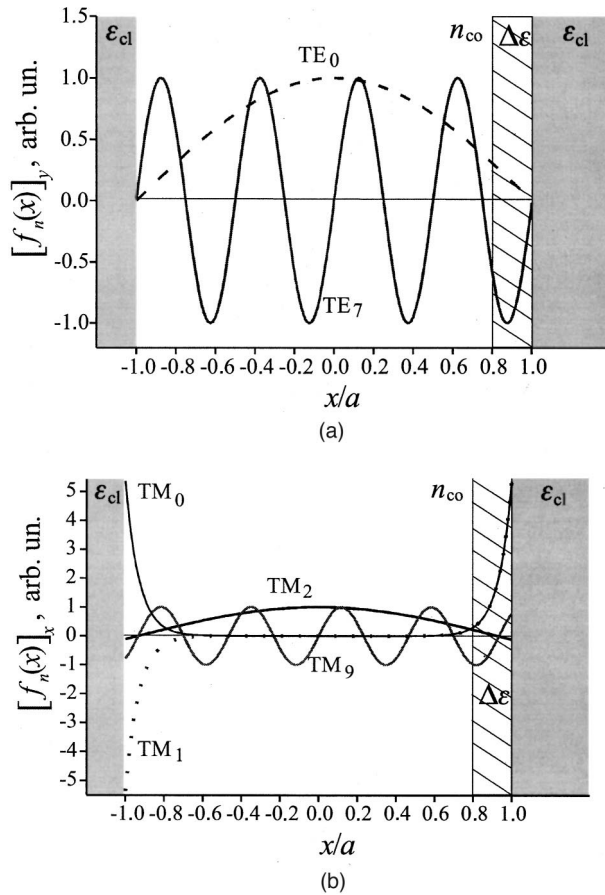


Fig. 3. Projections of the mode field amplitude (a) on the  $y$  axis,  $[f_n(x)]_y$ , for the  $TE_0$  and  $TE_7$  modes and (b) on the  $x$  axis,  $[f_n(x)]_x$ , for the  $TM_0$ ,  $TM_1$ ,  $TM_2$ , and  $TM_9$  modes of a planar waveguide with aluminum-coated walls for  $a = 11 \mu\text{m}$ ,  $n_{co} = 1$ ,  $\lambda = 0.62 \mu\text{m}$ ,  $\text{Re}(\epsilon_{cl}) = -54$ , and  $\text{Im}(\epsilon_{cl}) = 20$ . The hatched area shows the region of nonzero perturbation of the dielectric function.

in the indices of coupled modes. Thus photonic bandgaps with a large magnitude and a large width can be expected in the case of a metal-coated corrugated waveguide when some forward TM mode is Bragg resonance coupled with a surface backward mode [Fig. 3(b)]. Photonic bandgaps with smaller amplitudes and widths may be also expected when forward modes are coupled with high-order backward modes [Fig. 3(a)].

We can rewrite Bragg condition (7) for the above-considered regimes of strong coupling in terms of the effective refractive index  $\tilde{n}_n = \beta_n/k$  as

$$\lambda \approx \frac{2\pi}{lG}(\tilde{n}_f + n_{co}) \quad (18)$$

in the area of photonic bandgap corresponding to a strong coupling of a forward TM mode with a backward surface TM mode [Fig. 3(b)] and

$$\lambda \geq \frac{2\pi}{lG}\tilde{n}_f \quad (19)$$

in the area of the photonic bandgap corresponding to a strong coupling of a forward TM mode with a high-order backward TM mode [Fig. 3(a)]. Deriving Eq. (18), we em-

ployed Eq. (9) and took into consideration that  $|\sqrt{\epsilon_{cl}}| \gg n_{co}$ . To obtain Eq. (19), we made use of the inequality  $\tilde{n}_b \ll 1$ , which is valid for high-order modes of metal-coated planar hollow waveguide.

#### 4. TRANSMISSION SPECTRA OF PLANAR HOLLOW PBG WAVEGUIDES

Guided by the idea of integrating a hollow waveguide and a PBG structure into a compact optical component, we created an optical element consisting of an aluminum-coated diffraction grating and an aluminum-coated mirror (or another diffraction grating). Our experiments were performed with 1200- and 2400-grooves/mm diffraction gratings, which allowed the photonic bandgaps to be observed in the visible range. The waveguiding length of the structure was equal to 6 cm. The separation between the grating and the mirror was varied from 20 up to 100  $\mu\text{m}$ . By changing this parameter, we were able to tune the photonic bandgap in transmission spectra of such structures (Fig. 4). To excite TE and TM modes in a planar PBG waveguide, we used incident light linearly polarized along the  $y$  and  $x$  axes, respectively (Fig. 1).

Transmission spectra of created planar hollow waveguides, as is seen from Fig. 4, feature photonic bandgaps, whose positions and parameters are sensitive to the polarization of probing radiation and characteristics of the waveguide. Physically, it is very instructive to adopt the attitude discussed in Sections 2 and 3 by thinking of the photonic bandgap arising in dispersion and transmission of such a structure as a region where forward and backward waves are strongly coupled to each other due to a Bragg resonance expressed by Eq. (7). The difference of transmission spectra for light with different polarizations is due to the difference in the dispersion of TE and TM modes, which, in addition, never talk to each other in our waveguide.

In the case of TM modes, the photonic bandgap around 0.73–0.76  $\mu\text{m}$  (see Fig. 4), can be attributed to a strong coupling of forward TM modes with backward surface modes. Propagation constants of waveguide modes in this case meet the phase-matching condition of Eq. (18), with one reciprocal lattice constant involved in momentum conservation,  $l = 1$ .

As one might expect from Eqs. (7) and (15), this photonic bandgap for TM-polarized light is blueshifted as the width of the waveguiding layer decreases (cf. Fig. 4). A decrease in  $a$  also leads to an increase in the magnitude and the width of the photonic bandgap, which is due to the growth in the degree of light localization within the area of perturbed dielectric function near the walls of the waveguide (Fig. 3), resulting in a stronger coupling of forward and backward modes.

Photonic bandgaps centered at 0.46  $\mu\text{m}$  in the case of TE-polarized light and 0.44  $\mu\text{m}$  in the case of TM-polarized light (Fig. 4) can be attributed to a strong coupling of forward waveguide modes with high-order backward modes. Propagation constants of coupled waveguide modes in this case are phase matched in accordance with Eq. (19), with one reciprocal lattice constant involved in momentum conservation. In perfect agreement with our expectations (see Section 3), these photonic

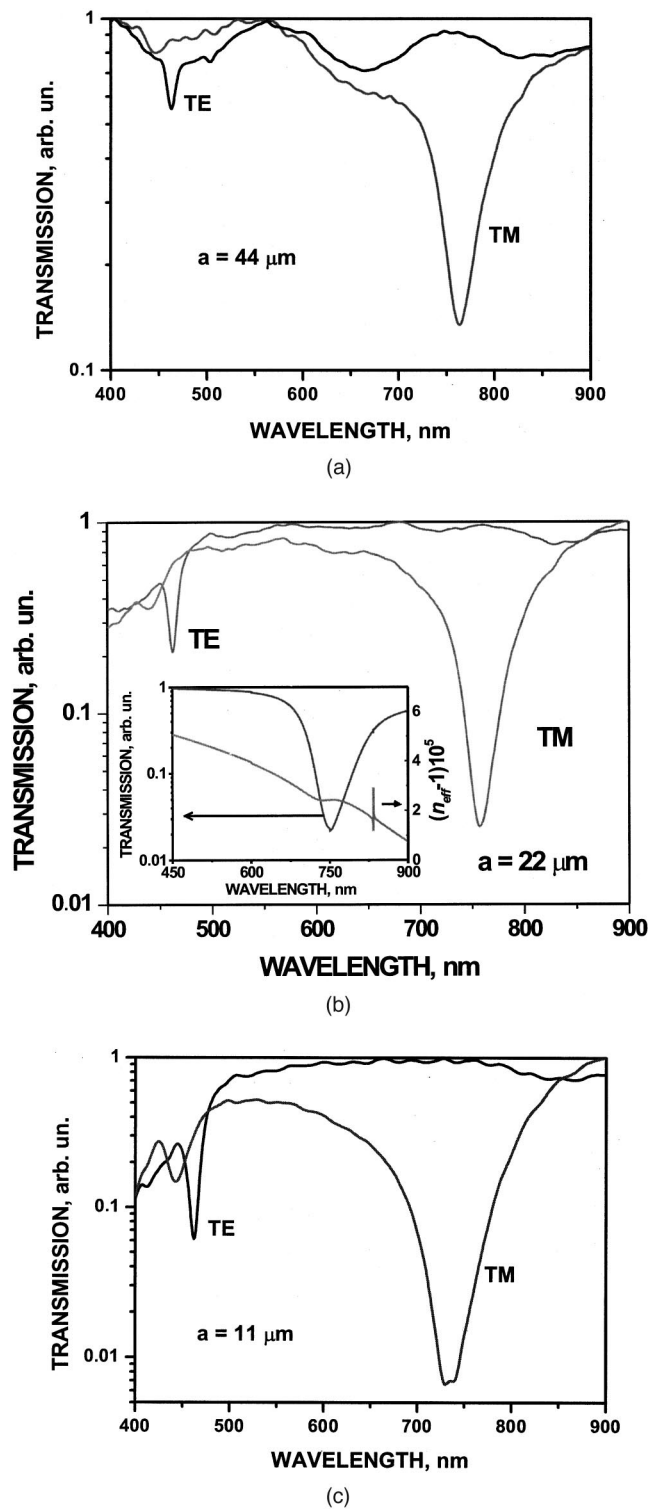


Fig. 4. Transmission spectra of a planar corrugated hollow waveguide consisting of a 2400-grooves/mm aluminum-coated grating and an aluminum mirror (see Fig. 1) with  $a$  equal to (a)  $44 \mu\text{m}$ , (b)  $22 \mu\text{m}$ , and (c)  $11 \mu\text{m}$ . The inset in Fig. 4(b) shows the results of calculations for the transmission spectrum and the spectral dependence of the effective refractive index for the  $\text{TM}_2$  mode coupled with the  $\text{TM}_0$  and  $\text{TM}_1$  modes.

bandgaps, related to a strong coupling of forward waveguide modes with high-order backward modes [Fig. 3(a)], have smaller depths and widths than the photonic band-

gaps corresponding to the coupling of a forward waveguide mode with backward surface TM modes [Fig. 3(b)].

To provide some idea of dispersion characteristics of the created PBG waveguide structure, the results of calculations for the transmission spectrum and the spectral dependence of the effective refractive index for the  $\text{TM}_2$  mode coupled with the  $\text{TM}_0$  and  $\text{TM}_1$  modes are presented in the inset to Fig. 4(b). The transmission spectrum shown in this inset qualitatively reproduces the bandgap observed in our experiments. The photonic bandgap appearing in both the transmission and refractive-index spectra corresponds to a strong coupling of the forward  $\text{TM}_2$  mode with backward  $\text{TM}_0$  and  $\text{TM}_1$  modes around a Bragg resonance with  $l = 1$ . Dispersion features related to the presence of the photonic bandgap offer several ways of increasing the efficiency of nonlinear optical processes in the waveguide of the considered type, allowing phase matching to be improved and local-field enhancement to be achieved. However, a detailed analysis of nonlinear optical interactions, such as self- and cross-phase modulation, as well as wave mixing and harmonic generation, requires a careful analysis of nonlinear propagation characteristics of light pulses in the created planar PBG waveguides, which falls beyond the scope of this paper.

In the context of nonlinear optical applications of the created PBG waveguide, the possibility of laser-induced damage of metallic mirrors and grating has to be taken into consideration. At high intensities of laser radiation, waveguide modes providing a high concentration of laser power in the waveguide core may become preferable. In particular, the ratio of the maximum field intensity in the waveguide core to the field intensity on the metal boundary for a planar aluminum-wall PBG waveguide with  $a = 11 \mu\text{m}$  is  $10^2$  for the  $\text{TM}_2$  mode and  $3 \times 10^5$  for the  $\text{TE}_0$  mode at the wavelength  $\lambda = 0.62 \mu\text{m}$ . This ratio can be further increased by use of PBG waveguides with, for example, silver-coated walls. This shows that, although the laser-induced damage of metal elements may sometimes lead to serious experimental difficulties, sufficiently high intensities of laser fields can be achieved in the core of the waveguide without inducing damage of waveguide walls with an appropriate choice of waveguide modes and, if necessary, the material of waveguide walls, as demonstrated by recent experiments on four-wave mixing in the gas phase enhanced with a waveguide of the above-described type.<sup>37</sup>

## 5. CONCLUSION

Thus the created optical component consisting of a metal-coated diffraction grating and a metal mirror combines dispersion properties of a hollow waveguide, a PBG structure, and a gas filling the gap between the grating and the mirror. Such structures display properties similar to the properties of planar corrugated waveguides, displaying, in particular, photonic bandgaps in the dispersion relation and transmission spectra due to a strong coupling of forward and backward waves within certain frequency ranges. However, in contrast to a conventional corrugated waveguide, the light is guided in a gas (or whatever fills the gap between the grating and the mirror) in our structure, which permits such structures to be employed

to waveguide high-intensity laser pulses, thus allowing many remarkable opportunities of gas-filled hollow waveguides demonstrated in the past few years by ultrashort-pulse generation and nonlinear optical frequency-conversion experiments to be considerably expanded.

Since the created waveguides display photonic bandgaps within the range accessible for many common lasers, including lasers generating short pulses, we believe that such structures may be very useful for many practical applications, including pulse compression based on self-phase modulation enhanced due to light-localization capabilities of the PBG structure, high-order harmonic generation with efficiency improved due to phase- and group-velocity matching and light localization, and nonlinear optical gas-phase analysis. With an appropriate choice of a resonant gas filling the gap between the grating and the mirror, such waveguide structures can be also used as optical filters whose transmission spectra may be tuned in a very practical way by simply changing the gas pressure.

## ACKNOWLEDGMENTS

We are grateful to S.O. Konorov for his help with computer simulations. The research described in this publication was made possible in part by Awards RP2-2266 and RP2-2275 of the U.S. Civilian Research and Development Foundation for the Independent States of the former Soviet Union. The work of A. B. Fedotov, A. N. Naumov, D. A. Sidorov-Biryukov, N. V. Chigarev, and A. M. Zheltikov was also supported in part by President of Russian Federation grant 00-15-99304, Russian Foundation for Basic Research project 00-02-17567, and Volkswagen Foundation project I/76 869.

## REFERENCES

1. E. Yablonovitch, "Photonic band-gap structures," *J. Opt. Soc. Am. B* **10**, 283–295 (1993).
2. C. Soukoulis, ed., *Photonic Band Gap Materials* (Kluwer Academic, Dordrecht, The Netherlands, 1996).
3. J. Joannopoulos, R. Meade, and J. Winn, *Photonic Crystals* (Princeton University, Princeton, N. J., 1995).
4. M. Born and E. Wolf, *Principles of Optics*, 6th ed. (Pergamon, Oxford, 1980).
5. H. Yokoyama, K. Nishi, T. Anan, H. Yamada, S. D. Brorson, and E. P. Ippen, "Enhanced spontaneous emission from GaAs quantum wells in monolithic microcavities," *Appl. Phys. Lett.* **57**, 2814–2816 (1990).
6. I. D. Jung, F. X. Kärtner, N. Matuschek, D. H. Sutter, F. Morie-Genoud, Z. Shi, V. Scheuer, M. Tilsch, T. Tschudi, and U. Keller, "Semiconductor saturable absorber mirrors supporting sub-10-fs pulses," *Appl. Phys. B* **65**, 137–150 (1997).
7. A. Y. Cho, A. Yariv, and P. Yeh, "Observation of confined propagation in Bragg waveguides," *Appl. Phys. Lett.* **30**, 471–472 (1977).
8. A. Yariv and P. Yeh, *Optical Waves in Crystals* (Wiley, New York, 1984).
9. S. S. Wang and R. Magnusson, "Multilayer waveguide-grating filters," *Appl. Opt.* **34**, 2414–2420 (1995).
10. G. Cerullo, M. Nisoli, S. Stagira, S. De Silvestri, G. Tempea, F. Krausz, and K. Ferencz, "Mirror-dispersion-controlled sub-10-fs optical parametric amplifier in the visible," *Opt. Lett.* **24**, 1529–1531 (1999).
11. O. Dühr, E. T. J. Nibbering, G. Korn, G. Tempea, and F. Krausz, "Generation of intense 8-fs pulses at 400 nm," *Opt. Lett.* **24**, 34–36 (1999).
12. N. I. Koroteev, S. A. Magnitskii, A. V. Tarasishin, and A. M. Zheltikov, "Compression of ultrashort light pulses in photonic crystals: when envelopes cease to be slow," *Opt. Commun.* **159**, 191–202 (1999).
13. M. Scalora, R. J. Flynn, S. B. Reinhardt, R. L. Fork, M. J. Bloemer, M. D. Tocci, C. M. Bowden, H. Ledbetter, J. Bendickson, J. P. Dowling, and R. P. Leavitt, "Ultrashort pulse propagation at the photonic band edge: Large tunable group delay with minimal distortion and loss," *Phys. Rev. E* **54**, R1078–R1081 (1996).
14. M. Scalora, M. J. Bloemer, A. S. Manka, J. P. Dowling, C. M. Bowden, R. Viswanathan, and J. W. Haus, "Pulsed second-harmonic generation in nonlinear, one-dimensional, periodic structures," *Phys. Rev. A* **56**, 3166–3174 (1997).
15. A. M. Zheltikov, A. V. Tarasishin, and S. A. Magnitskii, "Phase and group-velocity matching in ultrashort-pulse second-harmonic generation in one-dimensional photonic crystals," *J. Exp. Theor. Phys.* **91**, 298–306 (2000).
16. M. Scalora, J. P. Dowling, C. M. Bowden, and M. J. Bloemer, "Optical limiting and switching of ultrashort pulses in nonlinear photonic band gap materials," *Phys. Rev. Lett.* **73**, 1368–1371 (1994).
17. P. Tran, "Optical switching with a nonlinear photonic crystal: a numerical study," *Opt. Lett.* **21**, 1138–1140 (1996).
18. P. Tran, "All-optical switching with a nonlinear chiral photonic bandgap structure," *J. Opt. Soc. Am. B* **16**, 70–73 (1999).
19. S. Scholz, O. Hess, and R. Ruhle, "Dynamic cross-waveguide optical switching with a nonlinear photonic band-gap structure," *Opt. Express* **3**, 28–34 (1998).
20. I. S. Nefedov, V. N. Gusyatinikov, P. K. Kashkarov, and A. M. Zheltikov, "Low-threshold photonic band-gap optical logic gates," *Laser Phys.* **10**, 640–644 (2000).
21. R. Szipöcs, K. Ferencz, Ch. Spielmann, and F. Krausz, "Chirped multilayer coatings for broadband dispersion control in femtosecond lasers," *Opt. Lett.* **19**, 201–203 (1994).
22. A. Stingl, M. Lenzner, Ch. Spielmann, F. Krausz, and R. Szipöcs, "Sub-10-fs mirror-dispersion-controlled Ti:sapphire laser," *Opt. Lett.* **20**, 602–604 (1995).
23. L. Xu, Ch. Spielmann, F. Krausz, and R. Szipöcs, "Ultrabroadband ring oscillator for sub-10-fs pulse generation," *Opt. Lett.* **21**, 1259–1261 (1996).
24. D. Kopf, A. Prasad, G. Zhang, M. Moser, and U. Keller, "Broadly tunable femtosecond Cr:LiSAF laser," *Opt. Lett.* **22**, 621–623 (1997).
25. E. J. Mayer, J. Mobius, A. Euteneuer, W. W. Ruhle, and R. Szipöcs, "Ultrabroadband chirped mirrors for femtosecond lasers," *Opt. Lett.* **22**, 528–530 (1997).
26. F. X. Kärtner, N. Matuschek, T. Schibli, U. Keller, H. A. Haus, C. Heine, R. Morf, V. Scheuer, M. Tilsch, and T. Tschudi, "Design and fabrication of double-chirped mirrors," *Opt. Lett.* **22**, 831–833 (1997).
27. M. Nisoli, S. De Silvestri, and O. Svelto, "Generation of high energy 10 fs pulses by a new pulse compression technique," *Appl. Phys. Lett.* **68**, 2793–2795 (1996).
28. M. Nisoli, S. De Silvestri, O. Svelto, R. Szipöcs, K. Ferencz, Ch. Spielmann, S. Sartania, and F. Krausz, "Compression of high-energy laser pulses below 5 fs," *Opt. Lett.* **22**, 522–524 (1997).
29. A. Rundquist, C. G. Durfee III, Z. Chang, C. Herne, S. Backus, M. M. Murnane, and H. C. Kapteyn, "Phase-matched generation of coherent soft x-rays," *Science* **368**, 1412–1415 (1998).
30. C. G. Durfee III, A. R. Rundquist, S. Backus, C. Herne, M. M. Murnane, and H. C. Kapteyn, "Phase matching of high-order harmonics in hollow waveguides," *Phys. Rev. Lett.* **83**, 2187–2190 (1999).
31. E. Constant, D. Garzella, P. Breger, E. Mevel, Ch. Dorrer, C. Le Blanc, F. Salin, and P. Agostini, "Optimizing high harmonic generation in absorbing gases: model and experiment," *Phys. Rev. Lett.* **82**, 1668–1671 (1999).
32. R. B. Miles, G. Laufer, and G. C. Bjorklund, "Coherent anti-

- Stokes Raman scattering in a hollow dielectric waveguide," *Appl. Phys. Lett.* **30**, 417–419 (1977).
33. A. B. Fedotov, F. Giammanco, A. N. Naumov, P. Marsili, A. Ruffini, D. A. Sidorov-Biryukov, and A. M. Zheltikov, "Four-wave mixing of picosecond pulses in hollow fibers: expanding the possibilities of gas-phase analysis," *Appl. Phys. B* **72**, 575–582 (2001).
  34. K. Todor and S. Hayase, "Formation of pseudo one-dimensional photonic band in visible region by grating pair method," *Appl. Phys. Lett.* **70**, 550–552 (1997).
  35. M. J. Adams, *An Introduction to Optical Waveguides* (Wiley, New York, 1981).
  36. A. W. Snyder and J. D. Love, *Optical Waveguide Theory* (Chapman & Hall, London, 1983).
  37. S. O. Konorov, D. A. Akimov, A. N. Naumov, A. B. Fedotov, R. B. Miles, J. W. Haus, and A. M. Zheltikov, "Coherent anti-Stokes Raman scattering of slow light in a hollow planar periodically corrugated waveguide," *JETP Lett.* **75**, 66–70 (2002).